



This item was submitted to Loughborough's Institutional Repository (<https://dspace.lboro.ac.uk/>) by the author and is made available under the following Creative Commons Licence conditions.



**CC creative commons**  
COMMONS DEED

**Attribution-NonCommercial-NoDerivs 2.5**

**You are free:**

- to copy, distribute, display, and perform the work

**Under the following conditions:**

**BY:** **Attribution.** You must attribute the work in the manner specified by the author or licensor.

**Noncommercial.** You may not use this work for commercial purposes.

**No Derivative Works.** You may not alter, transform, or build upon this work.

- For any reuse or distribution, you must make clear to others the license terms of this work.
- Any of these conditions can be waived if you get permission from the copyright holder.

**Your fair use and other rights are in no way affected by the above.**

This is a human-readable summary of the [Legal Code \(the full license\)](#).

[Disclaimer](#) 

For the full text of this licence, please go to:  
<http://creativecommons.org/licenses/by-nc-nd/2.5/>

# Simple determination of the axial stiffness for large-diameter independent wire rope core or fibre core wire ropes

M Raouf\* and T J Davies

Civil and Building Engineering Department, Loughborough University, Loughborough, Leicestershire, UK

**Abstract:** Raouf and Kraincanic recently developed two somewhat different theoretical models for analysing large-diameter wire ropes with either an independent wire rope core (IWRC) or a fibre core. Most importantly, unlike all of the previously available theories (with their often very lengthy mathematical formulations), very encouraging correlations have been found between Raouf and Kraincanic's theoretical predictions of wire rope axial stiffnesses and a fairly large body of experimental data from other sources, hence providing ample support for the reliability of both theoretical models. Raouf and Kraincanic's original models were, however, computer based and involved certain iterative procedures. This potential drawback for practical applications (in an area where, by tradition, the rule of thumb reigns supreme) is overcome in the present paper, which reports details of some simplified (but still accurate) procedures for predicting the no-slip and/or full-slip axial stiffnesses of wire ropes with either an independent wire rope core or a fibre core, with the proposed formulations being amenable to simple hand calculations using a pocket calculator, which is of value to busy practising engineers.

**Keywords:** wire ropes, friction, axial stiffness, bridges, offshore structures

## NOTATION

		$\alpha_i$	lay angle of layer $i$ in a strand with the king wire being layer number 1
$A_{Li}$	total cross-sectional area of the wires in layer $i$ of a strand	$\beta_j$	lay angle of a strand in layer $j$ of the wire rope
$A_w$	cross-sectional area for an individual round wire		
$d_w$	diameter of round wires		
$E_{\text{full-slip}}, E_{\text{no-slip}}$	full-slip and no-slip axial stiffnesses respectively of a wire rope based on the orthotropic sheet theory		
$E_{\text{rope}}$	wire rope's effective axial stiffness based on Hruska's approach		
$E_{\text{steel}}$	Young's modulus for steel		
$H$	Hruska's parameter = $E_{\text{rope}}/E_{\text{steel}}$		
$M$	total number of strands in a wire rope		
$n$	total number of layers of wires in a strand including the king wire (layer number 1)		
$n_w$	number of wires in a layer of spiral strand		

## 1 INTRODUCTION

During the past two decades or so, considerable interest has been shown in the mechanical characteristics of helically wound steel cables (spiral strands and/or wire ropes) for use in both onshore and offshore applications. At this point, it is probably worthwhile explaining the main difference between a spiral strand and a wire rope. A spiral strand is a group of wires laid helically in successive layers over a central straight king wire (or equal lay core), while a wire rope consists of (typically) six strands laid helically over a central core which may itself consist of a smaller independent wire rope (IWRC) or twisted fibres (FC) (Fig. 1). Wire ropes and/or spiral strands are used extensively in bridge design and as tension members for suspended and stayed structures generally. With reference to the offshore industry, there has been a growing need for longer and stronger cables,

The MS was received on 3 June 2003 and was accepted after revision for publication on 12 August 2003.

\* Corresponding author: Civil and Building Engineering Department, Loughborough University, Loughborough, Leicestershire LE11 3TU, UK.

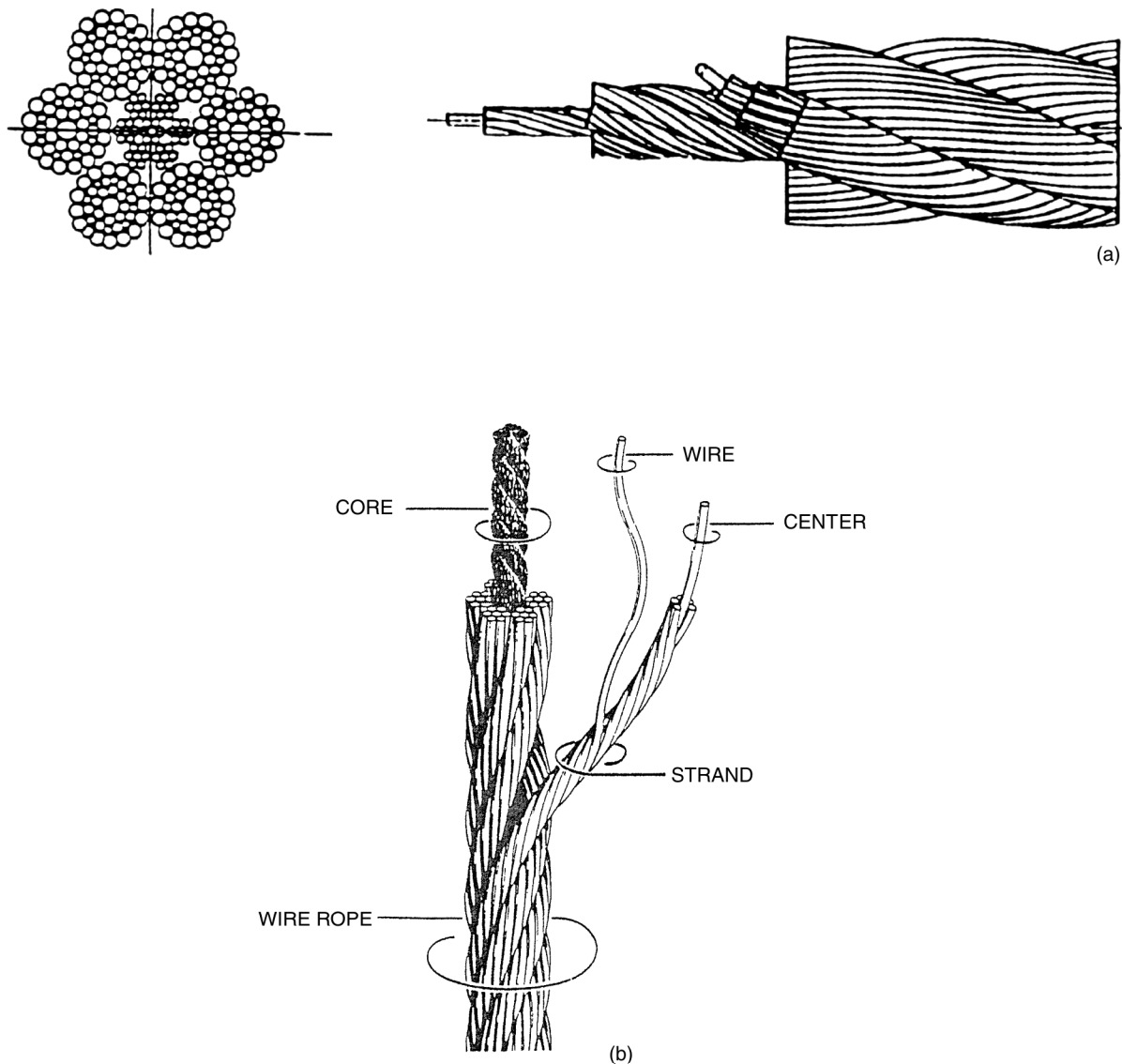


**Fig. 1** A typical six-stranded wire rope with: (a) an independent wire rope core (IWRC) (after Lee [8]) and (b) a fibre core (after Velinsky [5])

with increasingly larger outside diameters, for use as components in mooring systems for, for example, oil exploration and production platforms. The decision as to whether a spiral strand or a wire rope should be used is dependent upon the intended type of application. Wire rope is a little more flexible axially than a spiral strand, but considerably more flexible in bending, which is why wire ropes are used as tractive elements over pulleys, winch drums and fairleads in mines and cable cars (among others).

As regards the mathematical modelling of wire ropes, back in the 1980s encouraging progress was made by Costello and his associates (e.g. references [1] to [3]), Velinsky [4, 5], Lee *et al.* [6] and Lee [7, 8]. All these theoretical developments for wire ropes have, however, ignored the important effects of interwire friction and contact deformations: both of these effects are fully

catered for by Raoof and Kraincanic [9], who have also demonstrated that, for example, Velinsky *et al.*'s [2] predictions of axial stiffness for wire ropes with an IWRC, which are based on largely the same basic assumptions as those adopted by Costello and his other associates (e.g. references [1] and [3]), are not supported by the carefully conducted large-scale experiments of Strzemiecki and Hobbs [10] on a 40 mm outside diameter wire rope with an IWRC, with the length of the specimens ranging from 2.9 to 7.16 m. Jiang [11] has also reported a frictionless theoretical model for wire ropes with an IWRC, the predictions of which are very close to those of the theoretical model proposed by Velinsky *et al.* [2], with both models suffering from similar limitations.

Raoof and Hobbs [12] have developed the orthotropic sheet theoretical model: this concept is capable of

predicting, with a good degree of accuracy, the mechanical characteristics of spiral strands under not just static monotonic loading (which, incidentally, is the type of loading the previously reported frictionless theoretical models have primarily been developed for) but also when the strands experience cyclic loading. The results from the orthotropic sheet concept were subsequently used by Raof and Kraincanic [9, 13] to develop two somewhat different theoretical models for analysing the various stiffness characteristics of wire ropes with either a fibre or an independent wire rope core.

As originally shown by Raof and Hobbs [12], in repeated (cyclic) loading regimes, due to the presence of interwire friction, the effective axial stiffness of axially preloaded spiral strands (with their ends fixed against rotation) varies (as a function of the externally applied axial load perturbations/mean axial load) between two limits. The axial stiffnesses for small axial load changes (cf. the mean axial load) were shown to be significantly larger than for large axial load changes (associated with which gross slippage takes place between the wires in the line contact) because, for sufficiently small external axial load disturbances and in the presence of interwire friction, the helical wires stick together and the axially preloaded cable will effectively behave as a solid rod (with allowance being made for the presence of gaps between the individual wires). The upper and lower bounds to the axial stiffnesses were, therefore, referred to as the no-slip and full-slip types respectively. The same terminology was also adopted by Raof and Kraincanic [9, 13] in their theoretical treatment of wire ropes, which, as experimentally demonstrated by Strzemiecki and Hobbs [10], also exhibit the limiting no-slip and full-slip axial stiffness characteristics, when experiencing cyclic axial load perturbations superimposed on a mean axial preload.

In another publication, Raof [14], based on the results from an extensive series of theoretical parametric studies using a wide range of large-diameter spiral strand constructions, in conjunction with Hruska's [15] simple formulations, presented straightforward routines, based on the orthotropic sheet model, for estimating the no-slip and full-slip axial moduli of axially preloaded spiral strands, with any construction details. Raof [14] also showed that, primarily because of the inclusion of the strands' diametral contractions in the orthotropic sheet theory, the estimates of full-slip axial stiffness based on this model are significantly lower than those based on Hruska's approach.

The original theoretical models of Raof and Kraincanic for wire ropes [9, 13], although being very reliable, suffer from the potential drawback of being mathematically rather complex. Developing simple routines, which are amenable to hand calculations using a pocket calculator, similar to those for spiral strands, as already reported by Raof [14], is therefore highly desirable and forms the purpose of the present paper. In

what follows, based on an extension of the work of Strzemiecki and Hobbs [10], in conjunction with numerical results based on Raof and Kraincanic's models [9, 13], simple formulations will be developed for estimating the no-slip and full-slip axial stiffnesses of wire ropes, with either a fibre or an independent wire rope core, which should prove of value to busy practising engineers.

## 2 SIMPLIFIED METHODS

### 2.1 Hruska's approach

The general form of Hruska's equation, proposed by Strzemiecki and Hobbs [10], for the determination of the axial stiffness of a wire rope,  $E_{\text{rope}}$ , is (in the present notation)

$$H = \frac{E_{\text{rope}}}{E_{\text{steel}}} = \frac{\sum_{j=1}^M \left( \sum_{i=1}^n A_{L_i} \cos^3 \alpha_i \right) \cos^3 \beta_j}{\sum_{j=1}^M \left( \sum_{i=1}^n A_{L_i} / \cos \alpha_i \right) / \cos \beta_j} \quad (1)$$

where  $E_{\text{steel}}$  is the Young's modulus of steel,  $M$  is the total number of strands in the rope,  $n$  is the total number of layers of wires in each strand (including the king wire),  $A_{L_i}$  is the total cross-sectional area of the wires (which can have different diameters, even in a given layer) in layer  $i$  of a strand (with the king wire being layer number 1),  $\alpha_i$  is the lay angle of layer  $i$  in a strand and  $\beta_j$  is the lay angle of a strand in layer  $j$  of the rope. It should be noted that the denominator in equation (1) is equal to the total net steel area in the wire rope's normal cross-section, with the shapes of individual round wires and spiral strands in the wire rope's normal cross-section being elliptical [9, 13] and the central (king) wire in each spiral strand having  $\alpha_1 = 0$ .

According to equation (1), the dominant parameters controlling the rope axial stiffness are the lay angles ( $\beta_j$ ) of the strands in the wire rope and also the lay angles ( $\alpha_i$ ) of the steel wires forming the individual spiral strands, with the parameter  $A_{L_i}$  also playing a role.

### 2.2 Parameters used in the calculations

The numerical data relating to both the no-slip and full-slip axial stiffnesses, based on the work of Raof and Kraincanic [9, 13], on a number of wire ropes with fibre or independent wire rope cores, has been used in what follows. The fibre core wire ropes had outside diameters of 9.53 and 40.5 mm and were analysed assuming both a regular lay (RL) and a Lang lay (LL) type of construction. A Lang lay rope is the type in which the

directions of the lay of the individual wires in the outer strands and that of the outer strands in the rope are the same. If the lay directions of the wires and the strands are the opposite of each other, then the rope is of a regular lay type. It should be noted that the 'Hruska' stiffnesses, as calculated by equation (1), are the same, regardless of the type of lay. The wire ropes with independent wire rope cores had outside diameters of 33, 40, 55.6 and 76 mm. Two 76 mm outside diameter wire ropes were used in the analysis: a reasonably fully bedded-in (comparator) wire rope and a new wire rope.

The results, after Raooof and Kraincanic [13], for the fibre core wire ropes have been obtained assuming two different patterns (cases) of interstrand contacts: case 1, where the strands in the wire rope are assumed to be just touching each other in line contact, in an unstressed condition, so that the interstrand contacts in the hoop direction (with a higher normal stiffness compared to that in the radial direction) govern the diametral contraction of the rope; and case 2, where the strands in the wire rope are assumed to be resting on the fibre core, in the presence of significant gaps between the adjacent strands, so that the wire rope experiences radial deformations due to fibre core compliance.

The exact details of the theoretical model, relating to each case of interstrand contacts in wire ropes with fibre cores, are reported by Raooof and Kraincanic [13]. Moreover, the construction details of the wire ropes used in the present work, in conjunction with the calculation details of the Hruska's axial stiffnesses, are given elsewhere [16]. Alternatively, the full construction details for the individual wire ropes may be found in references [2], [10] and [17] to [19].

## 2.3 Results

Table 1 presents a summary of the final estimates of the axial stiffnesses, based on Hruska's approach, for each of the seven different wire rope constructions, as well as the numerical results for both the no-slip and full-slip axial stiffnesses, as reported by Raooof and Kraincanic [9, 13] and later on by Kraincanic and Hobbs [17], based on the considerably more complex (although more accurate) models of Raooof and Kraincanic [9, 13]. Table 2, as a typical example, gives the full construction details and calculation routines for Hruska's axial stiffness prediction of the 76 mm (comparator) outside diameter wire rope with an IWRC. The calculation routines for Hruska's axial stiffness,  $H$ , of wire ropes with fibre cores are exactly the same as those for wire ropes with an IWRC, with the proviso that in the former the contribution of the fibre core to axial stiffness,  $H$ , is assumed to be zero; i.e. only the contributions from the outer strands should be included. The predictions of wire rope axial stiffness in Table 1 are all based on the total net steel area [9, 13], the values of which for the individual wire ropes are also included in the last column of this table. Table 3, on the other hand, presents values of the corresponding experimentally determined axial stiffnesses, where available, as well as the ratios of predicted/experimental results (for  $E_{\text{no-slip}}$  and  $E_{\text{full-slip}}$ ) with the predictions (as given in Table 1) of  $E_{\text{no-slip}}$  and  $E_{\text{full-slip}}$  based on Raooof and Kraincanic's models for wire ropes with an IWRC or fibre core; the correlations between theory (which assumes a constant  $E_{\text{steel}} = 200 \text{ kN/mm}^2$  for all the wire rope constructions studied) and experiments are very encouraging. In particular, it is important to note that for the two types

**Table 1** Summary of the numerical results for the axial stiffnesses as calculated using Hruska's simple formula and the models proposed by Raooof and Kraincanic ( $E_{\text{steel}} = 200 \text{ kN/mm}^2$ )

Type of core construction*	Rope outside diameter (mm)	Hruska $E_{\text{rope}}/E_{\text{steel}}$	Raooof and Kraincanic			Total net steel area (mm <sup>2</sup> )
			$E_{\text{no-slip}}/E_{\text{steel}}$	$E_{\text{full-slip}}/E_{\text{steel}}$	$E_{\text{no-slip}}/E_{\text{full-slip}}$	
IWRC	33	0.657	0.561	0.478	1.174	518.46
IWRC	40	0.685	0.623	0.537	1.158	838.56
IWRC	55.6	0.802	0.779	0.714	1.092	1633.91
IWRC	76	0.754	0.708	0.646	1.096	3032.95
IWRC	76 (comparator)	0.718	0.654	0.583	1.122	2881.90
Case 1						
FC (RL)	9.53	0.701	0.714	0.654	1.092	39.65
FC (RL)	40.5	0.760	0.778	0.729	1.068	689.96
FC (LL)	9.53	0.701	0.701	0.636	1.102	39.65
FC (LL)	40.5	0.760	0.763	0.708	1.077	689.96
Case 2						
FC (RL)	9.53	0.701	0.658	0.608	1.081	39.65
FC (RL)	40.5	0.760	0.732	0.689	1.063	689.96
FC (LL)	9.53	0.701	0.652	0.600	1.086	39.65
FC (LL)	40.5	0.760	0.722	0.675	1.069	689.96

\* FC, fibre core; LL, Lang's lay; RL, regular lay.

**Table 2** Construction details and calculation routines for Hruska's axial stiffness of the 76 mm (comparator) outside diameter (IWRC) wire rope [ $(E_{\text{rope}}/E_{\text{steel}})_{\text{full-slip}} = 2068.407/2881.899 = 0.7177$ ]

1 Layer in the rope	2 Number of strands N	3 $\beta_j$ (deg)	4 Layer in the strand	5 $n_w$ wires	6 $d_w$ (mm)	7 $A_w$ (mm <sup>2</sup> )	8 $\alpha_i$ (degrees)	9 $n_w A_w / \cos \alpha_i$	10 $n_w A_w \times \cos^3 \alpha_i$	11 $N \times \sum (9) /$ $\cos \beta_j$	12 $N \times \sum (10) \times$ $\cos^2 \beta_j$
Core (1)	1	0	Core (1)	1	3.9	11.946	0	11.946	11.946		
King strand			2	6	3.54	9.842	14.84	61.091	53.339		
							Totals	73.037	65.285	73.037	65.285
IWRC strands (2)	6	18.11	Core (1)	1	3.34	8.762	0	8.762	8.762		
			2	6	3.1	7.548	14.84	46.849	40.904		
							Totals	55.610	49.666	351.052	255.864
Outer strands (3)	6	18.24	Core (1)	1	5.8	26.421	0	26.421	26.421		
			2	8	3.5	9.621	-9.53	78.046	73.826		
			3	8	2.4	4.524	-13.91	37.285	33.100		
			4	16	3.2	8.042	-13.07	66.051	59.468		
					3.7	10.752	-18.35	181.250	147.102		
							Totals	389.052	339.917	2457.810	1747.257
									Grand totals	2881.899	2068.407

**Table 3** Summary of the experimentally determined results for the axial stiffnesses of the various wire rope constructions

Type of core construction	Rope diameter (mm)	Source of experimental results	Experimental results			Predicted/experimental <sup>†</sup>	
			$E_{\text{no-slip}}^*/$ $E_{\text{steel}}$	$E_{\text{full-slip}}^*/$ $E_{\text{steel}}$	$E_{\text{no-slip}}/$ $E_{\text{full-slip}}$	For $E_{\text{full-slip}}$	For $E_{\text{no-slip}}$
IWRC	33	Velinsky <i>et al.</i> [2]	—	0.530	—	0.90	—
IWRC	40	Strzemiecki and Hobbs [10]	0.625	0.545	1.146	0.99	0.997
IWRC	76	Kraincanic and Hobbs [17]	0.685	0.653	1.049		
			0.722	0.678	1.065		
			0.723	0.652	1.109		
			0.819	0.663	1.235		
	Average		0.738	0.662	1.115	0.96	0.98
IWRC	76 (comparator)	Raooof and Kraincanic [18]	—	0.566	—	1.03	—
Case 1							
FC (RL)	9.53	Velinsky [5]	—	0.692	—	0.95	—
FC (RL)	40.5	Cantin <i>et al.</i> [19]	—	—	—	—	—
FC (LL)	9.53	Velinsky [5]	—	—	—	—	—
FC (LL)	40.5	Cantin <i>et al.</i> [19]	—	0.730–0.794	—	0.93	—
Case 2							
FC (RL)	9.53	Velinsky [5]	—	0.692	—	0.88	—
FC (RL)	40.5	Cantin <i>et al.</i> [19]	—	—	—	—	—
FC (LL)	9.53	Velinsky [5]	—	—	—	—	—
FC (LL)	40.5	Cantin <i>et al.</i> [19]	—	0.730–0.794	—	0.88	—

\* Assumed  $E_{\text{steel}} = 200 \text{ kN/mm}^2$ .<sup>†</sup> In connection with the experimental results with some reported scatter, the mean of the test results has been used.

of wire ropes with an IWRC for which the measured values of both the  $E_{\text{no-slip}}$  and  $E_{\text{full-slip}}$  are available, the correlations between the theory and test data (as regards both the upper and lower bounds to the wire rope axial stiffness) are, indeed, excellent, reinforcing the fact that such remarkable correlations are not due to mere coincidence (i.e. by chance); in other words, the presently assumed value of  $E_{\text{steel}} (= 200 \text{ kN/mm}^2)$  has not been used as a convenient fiddle factor.

Similar to the findings of Raooof [14] in the context of spiral strands, in Raooof and Kraincanic's models for wire ropes [9, 13], unlike the no-slip axial stiffness which is slightly dependent on the value of mean axial load, the full-slip axial stiffness is, in general, independent of the mean axial load, with both of these limiting (i.e. upper and lower bounds) values of axial stiffness being independent of the magnitude of the interwire coefficient of friction.

Furthermore, it is, perhaps, worth mentioning that the values of axial stiffness as traditionally quoted by the manufacturers, based on their shop measurements, are invariably the full-slip ones (in the present terminology), because of the large axial load ranges involved.

Figures 2 and 3 show the relationship between the full-slip axial stiffnesses as calculated using the simple formula of Hruska and Raooof and Kraincanic's [9, 13] models for all of the different wire rope constructions, relating to the results of cases 1 and 2 for the ropes with fibre cores respectively. Figure 4 shows similar correlations, but with the data relating to the fibre core wire ropes omitted.

Figures 5 and 6 present the relationships between the  $E_{\text{full-slip}}/E_{\text{steel}}$  and the  $E_{\text{no-slip}}/E_{\text{full-slip}}$  ratios, as calculated using Raooof and Kraincanic's [9, 13] models for wire ropes with fibre cores (cases 1 and 2 respectively) or

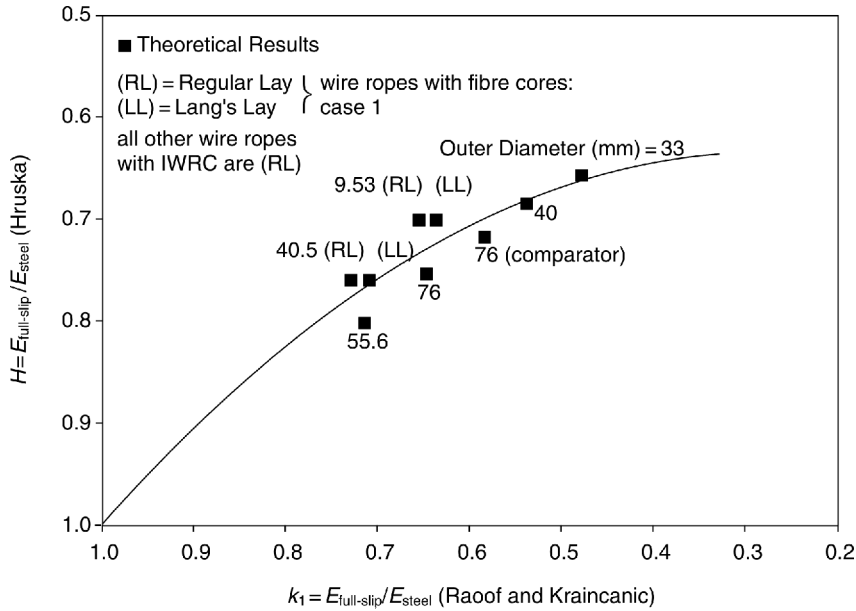


**Fig. 2** Relationship between the full-slip  $E$  values for various wire rope constructions with either a fibre core (case 1) or an IWRC as calculated using Raooof and Kraincanic's models and Hruska's formula

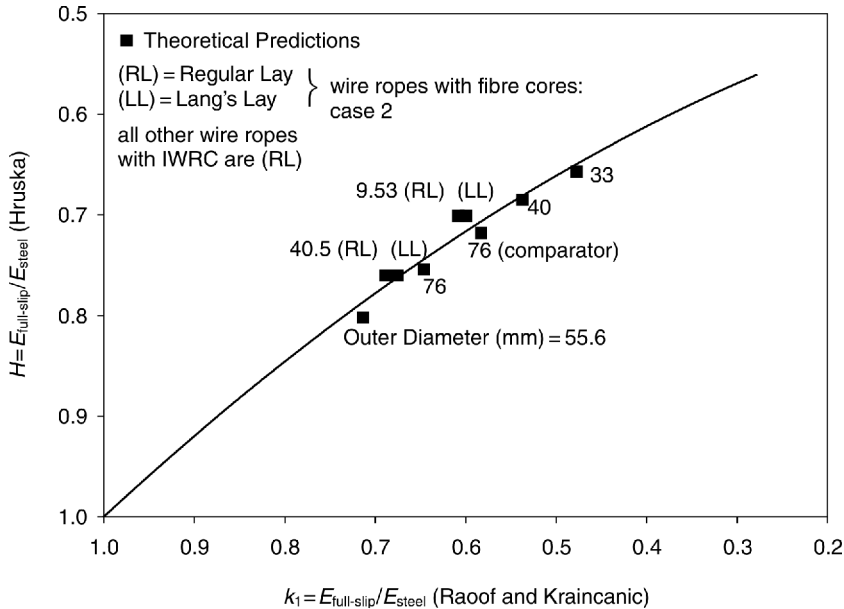


**Fig. 3** Relationship between the full-slip  $E$  values for various wire rope constructions with either a fibre core (case 2) or an IWRC as calculated using Raooof and Kraincanic's models and Hruska's formula

an IWRC. Figure 7 presents similar correlations, but with the data relating to the fibre core wire ropes omitted.

**2.4 Simple formulations**

Using the results presented in the previous section, a simple method for determining the full-slip and no-slip axial stiffnesses of wire ropes with either fibre cores or an IWRC can be developed by fitting various non-linear

curves (defined by second-order polynomials) through the data. In Figs 2, 3 and 4, Hruska's simple parameter  $H$  is given by equation (1), as developed by Strzemiecki and Hobbs [10]. Once  $H$  is calculated, the full-slip axial stiffness, based on the more accurate models of Raooof and Kraincanic, may be found using a second-order polynomial of the general form

$$\frac{E_{full-slip}}{E_{steel}} = A(H^2) + B(H) + C \tag{2}$$

where the constant coefficients  $A$  to  $C$  are given in

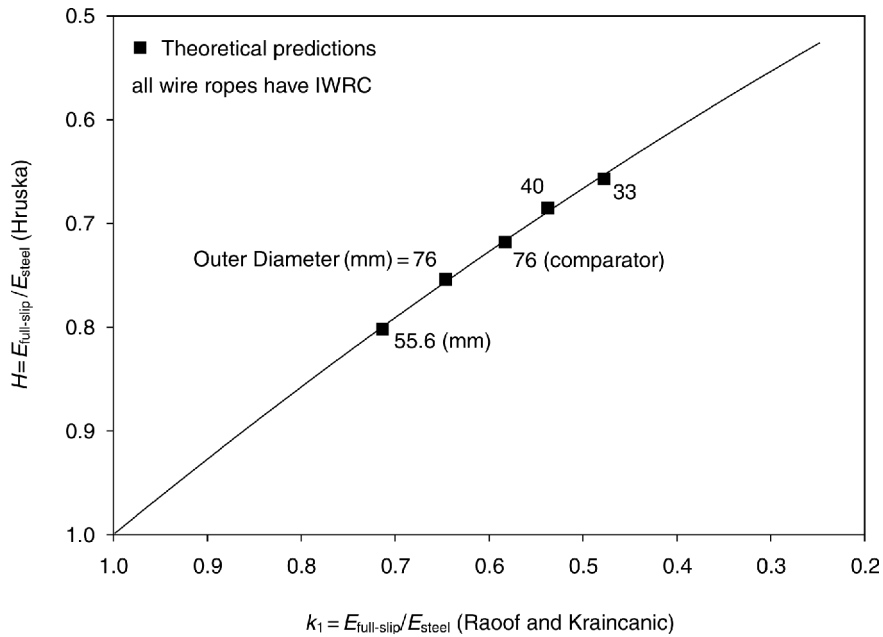


**Fig. 4** Relationship between the full-slip  $E$  values for the wire ropes with an IWRC as calculated using Raooof and Kraincanic's model and Hruska's formula

**Table 4** Values of the constant coefficients  $A$  to  $C$  in equation (2) for all of the fitted curves in Figs 2, 3 and 4, along with the correlation coefficients,  $R$

Reference	$A$	$B$	$C$	$R$
Fig. 2	-0.9099	2.9095	-1.00	0.870
Fig. 3	-0.6275	2.4872	-0.86	0.957
Fig. 4	-0.4913	2.3228	-0.83	0.998

Table 4 and correspond to the situation as to whether the fibre core wire ropes are to be included (Figs 2 and 3) or not (Fig. 4), and, if included, which different pattern of interstrand contacts for the ropes with fibre cores (i.e. whether case 1 or 2, as defined previously) is to be considered.

Turning to the no-slip case, Figs 5, 6 and 7 show the theoretical relationships between the no-slip and full-slip

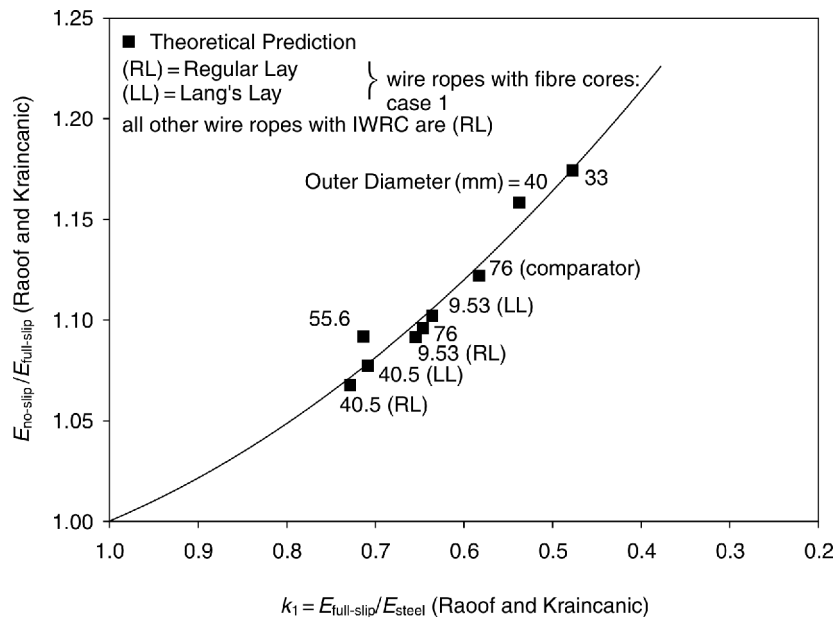


**Fig. 5** Relationship between the full-slip and no-slip  $E$  values for various wire rope constructions with either a fibre core (case 1) or an IWRC as calculated using Raooof and Kraincanic's models



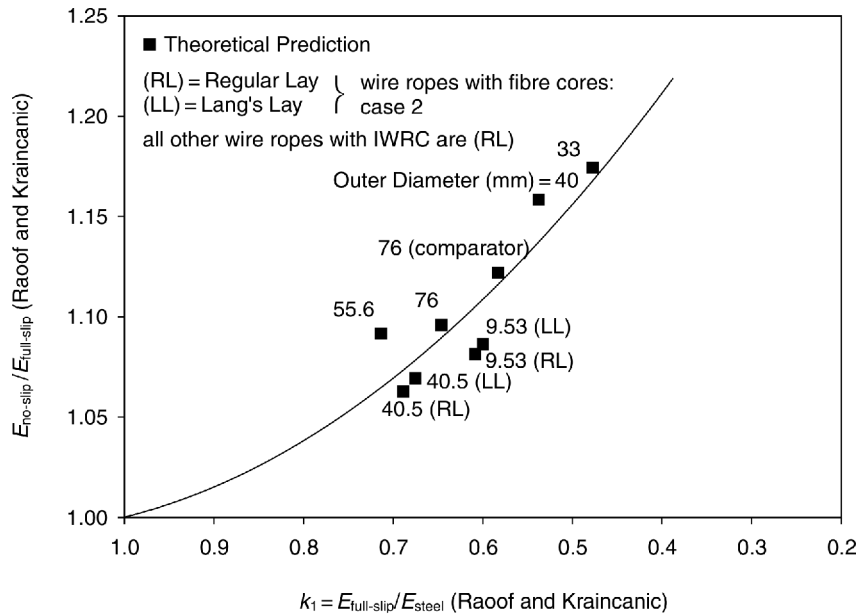


**Fig. 6** Relationship between the full-slip and no-slip  $E$  values for various wire rope constructions with either a fibre core (case 2) or an IWRC as calculated using Raof and Kraincanic’s models

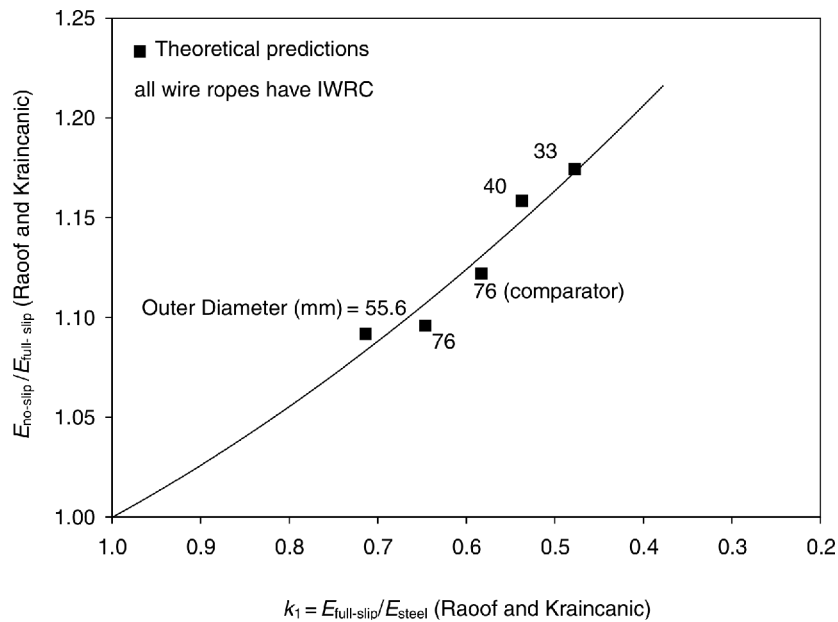


**Fig. 7** Relationship between the full-slip and no-slip  $E$  values for various wire rope constructions with IWRC as calculated using Raof and Kraincanic’s model

moduli, with the individual numerical results having been found to be very nearly independent of the level of mean axial load on the cable (over the working load ranges). Denoting  $E_{full-slip}/E_{steel} = k_1$ , fitted curves defined by second-order polynomials of the general form

$$\frac{E_{no-slip}}{E_{full-slip}} = E(k_1^2) + Fk_1 + G \quad (3)$$

provide a simple means of finding the no-slip axial

stiffness, once the corresponding full-slip axial stiffness has been found, depending upon whether the fibre core wire ropes are to be included (Figs 5 and 6) in the analysis or not (Fig. 7), and, if included, whether case 1 or 2 is to be adopted for the pattern of interstrand contacts in relation to the wire ropes with fibre cores. The values of the constant coefficients  $E$  to  $G$  in equation (3) are given in Table 5, along with the correlation coefficients,  $R$ .

**Table 5** Values of the constant coefficients  $E$  to  $G$  in equation (3) for all of the fitted curves in Figs 5, 6 and 7, along with the correlation coefficients,  $R$ 

Reference	$E$	$F$	$G$	$R$
Fig. 5	0.2855	-0.7563	1.471	0.9763
Fig. 6	0.4043	-0.9180	1.514	0.8893
Fig. 7	0.1656	-0.5759	1.410	0.9654

### 3 DISCUSSION

Similar to the results for spiral strands, based on the orthotropic sheet theory, the results for the axial stiffnesses of wire ropes with either fibre cores or an IWRC, based on Raof and Kraincanic's models, were found to give significantly lower  $E_{full-slip}$  values than those based on Hruska's simple approach, with the lay angles playing a primary (controlling) role.

Comparing Figs 2 and 3, it is found that the theoretical data are less scattered around the fitted curve when the fibre core wire ropes are analysed assuming that the strands in the wire rope are resting on the fibre core (case 2), in contrast to the situation when the strands in the wire rope are assumed to be just touching each other in the line contact (case 1). On the other hand, the opposite is found when comparing Figs 5 and 6, where the scatter of the data points about the fitted curves is less for case 1 (cf. case 2) of interstrand contacts in wire ropes with a fibre core.

With the data for the fibre core wire ropes omitted from the plots, the degree of scatter around the fitted curves is significantly less (refer to Fig. 4 and Fig. 7) with the fitted mean curve(s) very nearly passing through all the theoretical data points, which cover a rather wide

range of wire rope diameters and lay angles. This, then, suggests that the wire rope axial stiffness is determined by the lay angles of the wires in the strands and of the strands in the rope, with the other geometrical parameters having a second-order effect.

Table 6 presents a comparison between the predictions based on the quick calculation methods and the experimental results that are available, where the correlations in the case of wire ropes with an IWRC are, indeed, very good. As regards the wire ropes with fibre cores, the correlations are reasonable. It should be noted that, strictly speaking, the theoretical models of Raof and Kraincanic have both been developed for *large*-diameter wire ropes: this is probably the underlying reason for the relatively larger discrepancies (cf. other cases in Table 6) between theory and test data for the smaller 9.53 mm diameter wire rope with a fibre core.

Finally, the question may arise as to the accuracy that is required in these stiffness calculations at the design stage when such large-diameter wire ropes are used in engineering applications. Because of the wide variety of their common types of application (each of which imposes its own peculiar requirements), the required accuracy very much depends on the intended type of application. For the present purposes, it perhaps suffices to say that the very accurate estimates of axial stiffness required for wire ropes with an IWRC in, for example, the field of structural engineering may now be obtained, with minimal effort, by using the fitted polynomials to the data in Figs 4 and 7. As far as wire ropes with fibre cores are concerned, however, what is commonly required in practice is a reasonable (as opposed to very accurate) estimate of their axial stiffness, and in this respect the accuracy of the presently proposed method(s) is certainly sufficient to meet such practical requirements.

**Table 6** Comparison between the predictions based on the quick calculation method(s) and the available experimental results

Type of core construction	Rope outside diameter (mm)	Experimental results		Predicted values (using the appropriate polynomials)		Figure numbers for the appropriate polynomials
		$E_{no-slip}/E_{steel}$	$E_{full-slip}/E_{steel}$	$E_{no-slip}/E_{steel}$	$E_{full-slip}/E_{steel}$ (= $k_1$ )	
IWRC	33	—	0.530	0.566	0.484	7 and 4
IWRC	40	0.625	0.545	0.611	0.531	
IWRC	76	0.738*	0.662*	0.712	0.642	
IWRC	76 (comparator)	—	0.566	0.660	0.584	
Case 1						
FC (RL)	9.53	—	0.692	0.665	0.592	5 and 2
FC (LL)	40.5	—	0.730–0.794	0.745	0.685	
Case 2						
FC (RL)	9.53	—	0.692	0.644	0.575	6 and 3
FC (LL)	40.5	—	0.730–0.794	0.722	0.668	

\* The average of the corresponding experimental data as given in Table 3.

## 4 CONCLUSIONS

Numerical data, based on Raouf and Kraincanic's models, have been used to produce simple design procedures in relation to the upper (no-slip) and lower (full-slip) bounds to the axial stiffness of wire ropes with either fibre or independent wire rope cores. Most importantly, unlike all of the previously available theories (with their often very lengthy mathematical formulations), the available experimental data on a wide range of wire rope constructions have been found to provide encouraging support for the present theoretical predictions which fully cater for the important effects (totally ignored in the previously available theories) of interwire friction and contact deformations.

The present work clearly demonstrates that, using the simple formulation of Hruska, higher values of the full-slip axial stiffness are obtained when compared to the more refined models of Raouf and Kraincanic. With this borne in mind, a simple method has been proposed by means of which the no-slip and full-slip axial stiffnesses of axially preloaded large-diameter wire ropes, with either a fibre core or an IWRC experiencing superimposed cyclic axial load perturbations, may be estimated. The proposed method, which can also handle the simpler case of static monotonic loading with its associated *constant* (full-slip) axial stiffness, is based on the remarkable correlations found between the predictions of the axial stiffnesses as obtained from Hruska's and Raouf and Kraincanic's approaches, strongly suggesting that the lay angles (both of the wires in the strands and the strands in the rope) are the prime (controlling) parameters, with the cross-sectional areas of the individual wires also playing a role. The presently proposed method is amenable to simple hand calculations, using a pocket calculator, and is hence of value to busy practising engineers using the wire ropes in both onshore and offshore applications, where (as far as wire ropes are concerned) by tradition the rule of thumb reigns supreme.

## REFERENCES

- 1 Costello, G. A. and Miller, R. E. Static response of reduced rotation rope. *J. Engng Mechanics Div., ASCE*, 1980, **106**(EM4), 623–631.
- 2 Velinsky, S. A., Anderson, G. L. and Costello, G. A. Wire rope with complex cross sections. *J. Engng Mechanics, ASCE*, March 1984, **110**(3), 380–391.
- 3 Phillips, J. W. and Costello, G. A. Analysis of wire ropes with internal-wire-rope cores. *Trans. ASME, J. Appl. Mechanics*, September 1985, **52**, 510–516.
- 4 Velinsky, S. A. General non-linear theory for complex wire rope. *Int. J. Mech. Sci.*, 1985, **27**(7/8), 497–507.
- 5 Velinsky, S. A. Analysis of fibre-core wire rope. *Trans. ASME, J. Energy Resources Technol.*, September 1985, **107**, 388–393.
- 6 Lee, W. K., Casey, N. F. and Grey, T. G. F. Helix geometry in wire rope. *Wire Industry*, August 1987, 461–468.
- 7 Lee, W. K. The mechanics and mathematical modelling of wire rope. PhD dissertation submitted to Strathclyde University, 1989.
- 8 Lee, W. K. An insight into wire rope geometry. *Int. J. Solids and Structs*, 1991, **28**(4), 471–490.
- 9 Raouf, M. and Kraincanic, I. Analysis of large diameter steel ropes. *J. Engng Mechanics, ASCE*, June 1995, **121**(6), 667–675.
- 10 Strzemiecki, J. and Hobbs, R. E. Properties of wire rope under various fatigue loadings. CESLIC Report SC6, Civil Engineering Department, Imperial College, London, 1988.
- 11 Jiang, W. A. A general formulation of the theory of wire ropes. *Trans. ASME, J. Appl. Mechanics*, September 1995, **62**, 747–755.
- 12 Raouf, M. and Hobbs, R. E. Analysis of multi-layered structural strands. *J. Engng Mechanics, ASCE*, July 1988, **114**(7), 1166–1182.
- 13 Raouf, M. and Kraincanic, I. Characteristics of fibre-core wire rope. *J. Strain Analysis*, 1995, **30**(3), 217–226.
- 14 Raouf, M. Simple formulae for spiral strands and multi-strand ropes. *Proc. Inst. Civ. Engrs, Part 2*, December 1990, **89**, 527–542.
- 15 Hruska, F. H. Calculation of stresses in wire ropes. *Wire and Wire Products*, September 1951, **26**, 766–767 and 799–801.
- 16 Davies, T. J. Static, dynamic and fatigue characteristics of helical cables. PhD thesis submitted to Loughborough University, December, 2000.
- 17 Kraincanic, I. and Hobbs, R. E. Axial stiffness and torsional effects in a 76 mm wire rope: experimental data and theoretical predictions. *J. Strain Analysis*, 1998, **34**(1), 39–51.
- 18 Raouf, M. and Kraincanic, I. Behaviour of large diameter wire ropes. *Int. J. Offshore and Polar Engng*, September 1996, **6**(3), 219–226.
- 19 Cantin, M. M., Cubat, D. and Nguyen Xuan, T. Experimental analysis and modelisation of the stiffness in torsion of wire ropes. In Proceedings of the Organisation Pour International l'Etude de l'Endurance des Cables (OIPPEC) Round Table Conference (Ed. L. Wiek), Delft University, The Netherlands, 1993, pp. II67–II77.